

# An Addressable Pneumatic Regulator for Distributed Control of Soft Robots

Joran W. Booth<sup>1,†</sup>, Jennifer C. Case<sup>1,2,†</sup>, Edward L. White<sup>2</sup>, Dylan S. Shah<sup>1</sup>, and Rebecca Kramer-Bottiglio<sup>1\*</sup>

**Abstract**—In this paper, we describe a digitally-controlled, miniature, multi-mode pressure regulator for integration directly into centimeter-scale soft robots. This regulator integrates best-of-class commercially-available pneumatic valves and pressure sensors to achieve a small and lightweight servo-controlled pressure regulator. We demonstrate that the regulator is able to track both step and ramp commands and quantify the error in the resulting pressure. In order to facilitate integration of many such regulators into a single soft robot, we have implemented an addressable digital communication system, based on the industry-standard I2C bus. This allows us to connect up to 127 regulators on a single 4-line bus, significantly reducing the mass and complexity of the required wiring.

## I. INTRODUCTION

Soft robots use low-modulus and multi-functional materials to create highly deformable robotic systems. The resulting systems possess many novel properties, such as light weight, robust structures, and the ability to operate in unstructured environments. The majority of research in the field to-date has focused on these novel structures, while comparatively little attention has been paid to the support elements which enable these capabilities. In the case of pneumatically-powered soft robots, pressure regulators are required to control the inflation of the actuators. The majority of current pneumatic robots use off-board pressure supplies and regulators and require a tether between the robot and the hardware. This strategy allows for the use of commercially-available pressure regulators, but limits the range and utility of the resulting robots.

An important goal for pneumatic soft robots is to have generalizable strategies for easily creating untethered robots. In this paper, we present a miniature pneumatic regulator capable of continuous pressure control, small enough to fit on centimeter-scale soft robots (Fig. 1). The regulators can operate in two modes: a servo-controlled mode for distributed closed-loop operation and an manual mode to enable off-board control. In servo-controlled mode, the regulator can be commanded to achieve a specific pressure. In manual mode, the regulator can be commanded to execute specific states, including fill, release, and hold, allowing the valves within the regulator to be activated from off-board. Each regulator is commanded over an addressable digital bus, enabling groups of regulators to achieve distributed control on a robotic body.

<sup>1</sup>School of Engineering & Applied Science, Yale University, New Haven, CT, USA

<sup>2</sup>School of Mechanical Engineering, Purdue University, West Lafayette, IN, USA

\*To whom correspondence should be addressed; E-mail: rebecca.kramer@yale.edu

<sup>†</sup>J.W. Booth and J.C. Case are co-first authors.

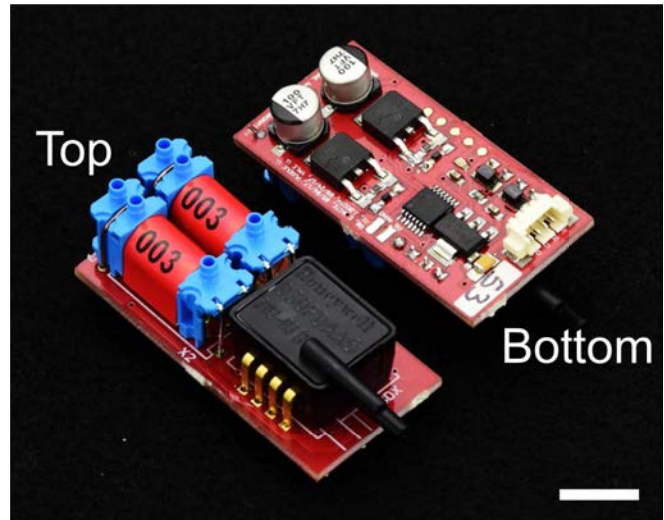


Fig. 1: The addressable pneumatic regulator. The regulator is able to imitate the function of a proportional valve, despite its compact size. By using the I2C protocol, the regulator is able to achieve distributed actuation while staying in a size small enough for centimeter-scale soft robots. The regulator measures 22 x 50 x 20 mm. The scale bar represents 1 cm.

This work advances the state of the art in soft robotics by simplifying valve control and distributed control in soft robots.

## II. BACKGROUND

Several groups have worked towards the goal of untethering pneumatically actuated soft robots. Tetherless robots have been created using several strategies. One strategy is to make the robot so large and correspondingly powerful, that it can lift its own power supply [1]. While this strategy is successful for meter-sized robots, the size and weight constraints of commercially available pneumatic components make it infeasible for smaller scales. Another strategy has the robot drag its power supply behind it on wheels [2], [3] or have an additional rigid robot carry the soft robot's power supply [4]. This strategy is good for testing robots, but may limit their use for in-field applications, such as search and rescue. An additional approach is to use chemical pressure generation, often through the decomposition of a monopropellant such as hydrogen peroxide [5]–[9] rather than to use an electrical air pump. This approach is easily scaled to centimeter-sized robots or smaller and is more weight efficient than a traditional pneumatic system. A final,

partial step, is to locate the control valves on the robot. Some research groups have incorporated miniature valves into their design [5], whereas others have created custom soft valves that are built into the robot body [5], [6], [9]. All these approaches are still nascent and have to be custom-designed for each new robot.

One problem with embedded valves, to date, is that they are limited to on-off functionality only. In addition, the embedded soft valves are driven by pressure gradients and current examples are passive and unable to be controlled by a central processor. While fluidic control has been demonstrated for a logic circuit [9] and as an addressable array of valves [10], each requires a highly customized system that is not generalizable. Further, fluidic control generally requires bulky and elaborate vascular systems for basic functions. It is unlikely that fluidic control will be a significant strategy for controlling pneumatic soft robots in the near-term. An additional problem with the current state-of-the-art is that large numbers of solenoid valves require complex wiring. Finally, all the examples of embedded valves discussed above use 2-way or 1-way valves. However, in many circumstances, it is desirable to hold a specific pressure in the actuator, which is why proportional valves are often used in off-board setups. Our approach to address these shortcomings is a miniaturized board capable of distributed control for variable pressure regulation.

### III. MATERIALS

The pneumatic regulator board is composed of a pressure sensor (Honeywell, ASDXRRX030PDAA5), two miniature 2-way valves (Parker X-valve, 912-000001-003), and a custom circuit board (see github link [11])

with an embedded microcontroller (Microchip, PIC16F1825T-I/ST). Firmware for the PIC and for an Arduino can also be found in [11]. The above pressure sensor and 2-way valves are limited to 207 kPa (30 psi). The resolution of the pressure sensor is 2% of the total range, which in the case shown in this paper is  $\pm 8.3$  kPa (1.2 psi). While the pressure sensors and 2-way valves demonstrated in this paper are limited to 207 kPa, we can achieve pressures up to 690 kPa (100 psi) by swapping the pressure sensor and valves with 100 psi versions (Honeywell ASDXRRX100PGAA5 and Parker 912-000001-021, respectively). The board uses I2C protocol to communicate with an external microcontroller (*e.g.*, Arduino, RaspberryPi). This architecture allows up to 127 regulators to connect to a single microprocessor. By using I2C protocol, only four lines are needed (power, ground, clock, and data), resulting in a simplified wiring harness for large numbers of regulators. The valves and pressure sensor are mounted on one side of the board, and the remaining circuit is mounted on the other side. The complete regulator assembly, including tubing, weighs 18 g. The regulator assembly is 22.2 mm x 49.5 mm x 20.0 mm without tubing. With tubing, it is about 22.2 mm x 56 mm x 30 mm, though this could be improved for a specific application.

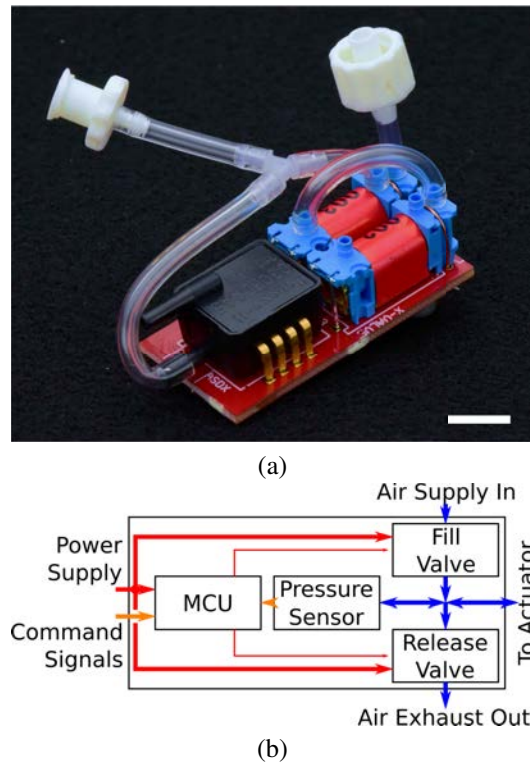


Fig. 2: (a) Photo and diagram showing how airflow occurs through the valves on the pressure regulator. The scale bar represents 1 cm. Alternate airflow configurations are possible with minimal changes to the firmware. (b) Schematic showing the functionality of the regulator.

The regulator is capable of replicating the function of a 3-way valve, which is not commercially available at the size of our modules. It does so by opening the first valve, which connects the supply in-line pressure to an actuator; closing both valves to hold the air in the actuator; and opening the second valve to release the air from the actuator to the atmosphere. A diagram of the port configuration is found in Fig. 2. The regulator can operate in two modes: manual and servo-controlled. In manual mode, the servo receives state commands (release, hold, or inflate) over the I2C communication lines and executes those states. Without the hold state, the system would need to alternate between fill and release to maintain a given pressure. The hold state reduces chatter and energy consumption and, thus, increases the lifetime of the regulator. Manual mode allows an external controller to actuate regulators, and may be used for open-loop control, or with an off-board logic controller that can be nested inside a feedforward or sensor-based control loop. In servo-controlled mode, an external microcontroller sends a desired pressure to the regulator over the I2C communication line. The regulator then uses the on-board sensor and logic controller to achieve the desired pressure. We implemented a simple bang-bang controller with a minimum deadband of 1 bit, which corresponds to 2 kPa. The sample frequency is constrained by the time it takes to operate each control loop,

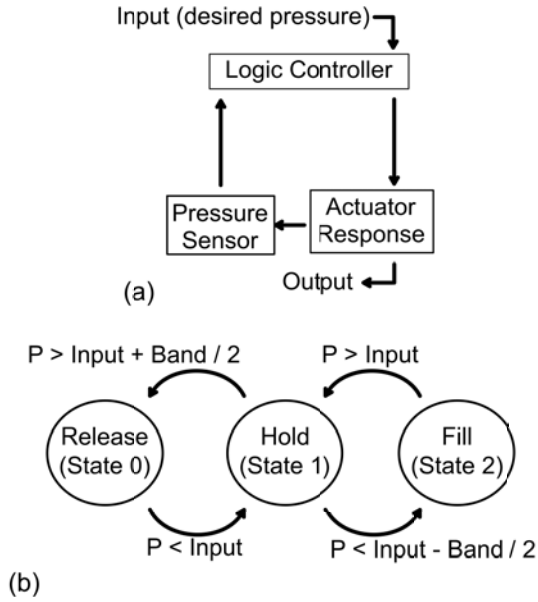


Fig. 3: (a) The control loop used by the on-board microprocessor when in servo-controlled mode. (b) The state machine used for the logic controller. When filling or releasing, the system stops and holds the pressure when the input pressure is crossed. However, it resumes filling or releasing if the pressure reading falls outside the band around the input pressure.

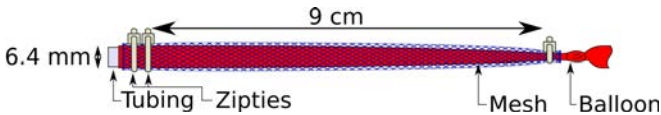


Fig. 4: Drawing of McKibben actuator with dimensions labeled.

and is 17.8 kHz. Fig. 3 shows the logic controller and state machine used by the on-board microprocessor. The following sections highlight the performance of the regulator in servo-controlled mode, since this allows for distributed control of multiple actuators.

#### IV. RESULTS & DISCUSSION

In order to highlight the utility of our pressure regulators, we first compare various parameters of our system to other existing pneumatic systems that have been reported. Additionally, we characterized the regulators looking at both system response and power consumption. We also show the system performance in terms of step and ramp inputs as well as response to disturbances. For our experiments, we used an in-line pressure of approximately 190 kPa and had a band of 2 bits on our servo-controlled pressure regulator, which corresponds to 4 kPa. Our characterization and system performance tests were done with a McKibben actuator that was 1 cm in diameter and 9 cm in active length when at rest, as seen in Fig. 4. Finally, we demonstrate these regulators on a five-actuator multi-gait soft robot [18].

#### A. Comparison

While many researchers do not report their pressure regulators, we compare our regulators to the fluidic control board reported on the Soft Robotics Toolkit website and the few reported hardware components we could find in the literature. This comparison is shown in Table I. Our pressure regulator is much smaller and lighter and performs the same number of functions or more than other reported systems.

#### B. System Characterization

1) *System Response*: We characterized the system response of the pneumatic regulator servo by measuring settling time, percent overshoot, and steady state error of the system using a McKibben actuator. Ten trials were collected at pressures ranging from 5 to 25 psi at 5 psi intervals (or 34, 69, 103, 138, 172 kPa). Each trial lasted 30 s. The settling time was defined to be how long it takes the system to reach and stay within 5% of the set point. The percent overshoot is found as the maximum value before the settling time. The steady state error is the set point minus the average pressure. This error was calculated using the average of the data after the system is considered settled via the calculated settling time. The results of the first second of these trials are shown in Fig. 5 and the settling times, percent overshoots, and steady state errors are presented in Table II.

The settling times for the McKibben actuator are all under 0.3 s. The settling times for the low pressures (34 and 69 kPa) were below 0.1 s. The settling time for the highest pressure (172 kPa) did not overshoot the desired pressure and, thus, the settling time is based on how long it takes to inflate to the desired pressure (0.17 s), which was very consistent, as can be seen in Fig. 5. This may be due to the fact that the pressure is close to the in-line pressure, which was chosen due to component limitations on the regulator. In contrast, the settling times for the 103 and 138 kPa trials were longer due to the system oscillating before coming to rest. We suspect that while filling at these intermediate pressures, the momentum of the air entering the actuator creates a shock-wave and resulting spike in pressure that is not sufficiently damped by the elasticity of the air or the actuator, similar to water hammer. An important consideration is that the settling time for actuators is limited by the pressure, flow-rate, and inflated volume of the actuator, which means that larger actuators will take a longer time to reach a desired pressure.

Looking at percent overshoot, we see that the lower pressures have larger overshoots than the higher pressures. We suspect this is due to the larger difference in the desired and in-line pressure for lower pressures. The steady state error shows that for all the pressures that we tested, we get errors within the range of the accuracy of the pressure sensor itself ( $\pm 8.3$  kPa). Therefore, the limitation in our regulators is due to the accuracy of the sensor rather than our controller.

2) *Power Consumption*: The power consumption of the pressure regulator depends on which state is active and is composed of two independent components: air and electrical power. The air power consumed by a robot depends on the

TABLE I: A comparison with other common pneumatic valve control systems used in soft robotics research. This comparison is not comprehensive since few research groups publish details on their off-board hardware. The Parker X-Valve is the same as on our regulator, but we include it in the comparison since it could be used independently. The Soft Robotics Toolkit (SRT) board includes more functions than our regulator provides, such as pressure generation, physical switches and an Arduino. We omit these elements when calculating the volume for this board.

Valve and Controller	Range	# Actuators	Package Volume	Flow Rate	Volume Specific		Weight	Control
					Flow Rate	Flow Rate		
Faboratory Regulator	0-207 kPa	1	22 cc/actuator	6.4 Lpm	290 s <sup>-1</sup>	18g	Logic	
Soft Robotics Toolkit [12]	0-700 kPa	4	770 cc/actuator	174 Lpm	226 s <sup>-1</sup>	-	PWM	
COTS Festo CPV 14-VI 18210 [13]	0-1000 kPa	6	236 cc/actuator	800 Lpm	3390 s <sup>-1</sup>	1530g	PLC	
COTS SMC ITV1031-21F1N-Q [14], [15]	0-500 kPa	1	244 cc/actuator	200 Lpm	818 s <sup>-1</sup>	350 g	PLC	
Valve Only								
COTS Parker X-Valve (207 kPa) [16]	0-207 kPa	1	2.2cc/actuator	6 Lpm	2730s <sup>-1</sup>	4.5g	N/A	
COTS Parker Ten-X (207 kPa) [1], [17]	0-207 kPa	1	9.6cc/actuator	12 Lpm	1250s <sup>-1</sup>	12g	N/A	

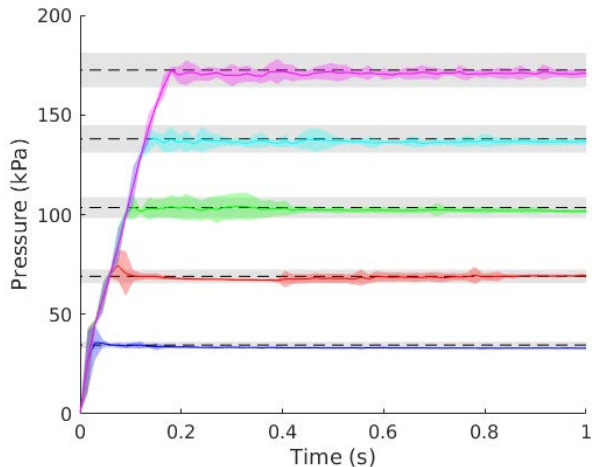


Fig. 5: System response for various pressures. The desired pressure is shown as black dashed lines with a 5% band shown in a gray cloud around the dashed line. The averaged response for 34 kPa is shown as blue; 69 kPa is shown as red; 103 kPa is shown as green; 138 kPa is shown as cyan; and 172 kPa is shown as magenta. The colored clouds around the averages represent 95% confidence intervals for 10 trials.

TABLE II: Characterization for 9 cm McKibben actuator at given desired pressures. Ten trials are used to calculate means and standard deviations.

Pressure (kPa)	Settling Time (s)	% Overshoot (%)	Steady State Error (kPa)
34	0.08 ± 0.04	10 ± 6	-0.0 ± 0.4
69	0.09 ± 0.01	12 ± 4	-1.0 ± 0.2
103	0.27 ± 0.12	6 ± 4	-1.2 ± 0.1
138	0.21 ± 0.14	3 ± 2	-1.5 ± 0.1
172	0.17 ± 0.00	0	-1.8 ± 0.1

TABLE III: Power characteristics for the pressure regulator, by state. Power expenditure due to air is not shown since it is dependent on the application and can be estimated with the flow rate.

State	Volts	Amps	Power
Hold	12V	0.022A	0.264W
Fill	12V	0.105A	1.26W
Release	12V	0.105A	1.26W

application, but can be easily estimated if the flow rate is known. As a result, we do not report power consumption due to air, but as an aid to future researchers we report the maximum flow rate that our regulator can achieve. In our experiments with the complete regulator assembly at room temperature, we measured a flow rate of 6.4 Lpm for 138 kPa over 10 trials using a 30 cm length of 3.2 mm (1/8") inner diameter (ID) tubing, but measured a flow rate of 4.7 Lpm when we used 90 cm length of 1.6 mm (1/16") ID tubing.

The electrical power consumed by the module is dependent on which state it is in. The regulator has three states: fill, hold, and release the air. The hold state consumes less power than the fill and release states. The fill and release states actuate a solenoid valve (X-Valve 912-000001-021, by Parker) which consumes 1 W when activated. The control board consumes 0.022 A, resulting in a power draw of 0.264 W. When in the hold state, the board consumes 0.264 W. When in the fill or release states, the regulator consumes 1.26 W. These results are summarized in Table III.

### C. System Performance

To demonstrate the capabilities of the regulator to follow commanded pressures, we tested the regulator using both step and ramp inputs. First, the regulator was commanded to hold each pressure (0, 34, 69, 103, 138, and 172 kPa) for 5 s stepping both up and down. Then the regulator was commanded to ramp up from 0 kPa to 172 kPa and back down over the course of 45 s. This procedure was done for 10 trials using our McKibben actuator. The results are shown in Fig. 6. This shows the capabilities of the regulator to not

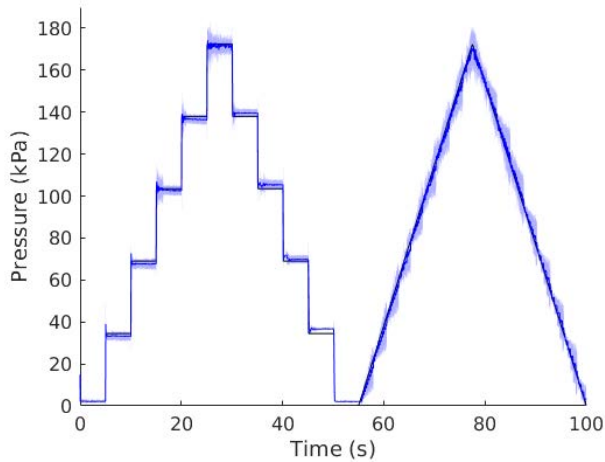


Fig. 6: Step and ramp responses of pressure regulator. The black line shows the desired pressure while the blue line shows the achieved pressure. The colored cloud around the average represent 95% confidence intervals for ten trials.

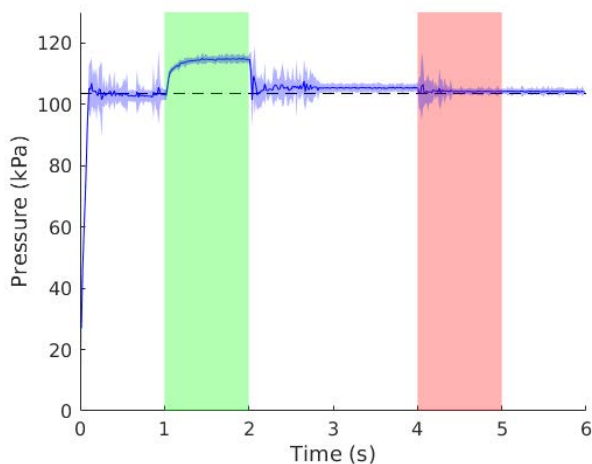


Fig. 7: Disturbance response of actuator (shown as the blue line) when exposed to approximately 190 kPa pressure for 1 s (green) and atmospheric pressure for 1 s (red). The blue clouds represent the 95% confidence intervals for 10 trials.

only hold a specific pressure, but to track desired pressure over time.

Because the logic controller is on-board, we are able to take advantage of the distributed control. The regulators are able to locally respond to disturbances, such as those caused by external conditions. To demonstrate this feature, we took our McKibben actuator and briefly exposed it to both 190 kPa and atmospheric pressure. In order to do this, we used two regulators that connected to the same actuator. One regulator was run in servo-controlled mode to maintain an actuator pressure of 103 kPa while the other regulator was run in manual mode to introduce the changes in pressure for 1 s intervals. Fig. 7 shows the regulator’s response to

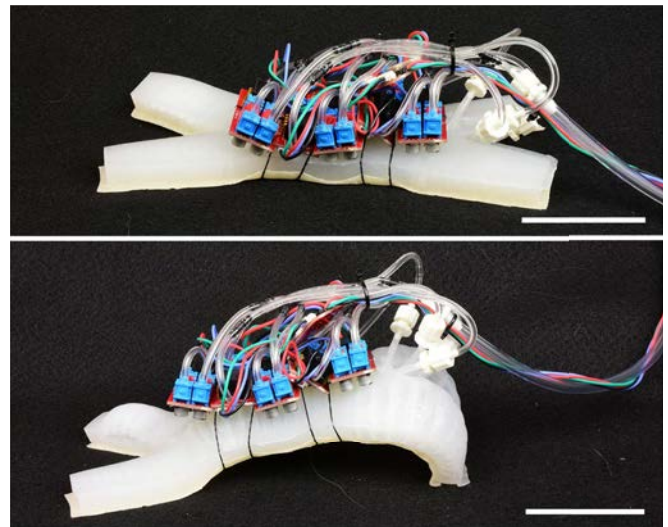


Fig. 8: Images of a soft locomotion robot with five regulators on board. Note that the tether consists of only one supply line and four wires. The scale bars represent 5 cm.

these disturbances for 10 trials. When the pressure increase was imposed on the actuator, the servo-controlled regulator was not able to fully compensate and we observed a pressure increase on the order of 10 kPa. This was because the airflow into the actuator from the manual regulator was higher than the airflow out from the servo-controlled regulator. The inflow rate and outflow rate are different in all pneumatic valves, so this behavior is expected. Further, the pressure plateaus, suggesting that the increased pressure and therefore increased inflow rate comes into equilibrium with the outflow rate. When we used the manual regulator to vent the actuator, we observed an immediate disturbance that quickly settled back to 103 kPa. The servo-controlled regulator fully compensated for the leaking. The results of this experiment demonstrate that the regulators are able to compensate for minor leaks in actuators and other disturbances.

#### D. Robot Application

In order to demonstrate the regulators on a soft robot, we have utilized the multi-gait soft robot design from Shepherd *et al.* [18]. We chose this robot because it has multiple actuators and is well-known. Previously, this robot (approximately 14 cm in length) required five pneumatic tethers going to off-board control of its four legs and central body. A larger scale version of this robot (approximately 65 cm in length) has been previously made untethered by having the robot itself carry its power supply [1]. In contrast, the robot we employ here is approximately 20 cm in length and requires only a single pneumatic tether and a set of four wires for communication with the regulators. To position our pressure regulators on-board the quadruped soft robot, we strapped the regulators onto its back, as seen in Fig. 8. While this regulator placement is non-ideal since it limits the inflation of the central actuator, we are still able to show that regulators control the inflation of the limbs (Fig. 8). Future robots that

use these regulators should consider the placement of the components and accommodate for them during the design of the robot.

One important case where our regulator design may be especially useful is in robot implementations where there is significant variability between actuators. For example, in the case of the multi-gait soft robot, each leg actuates to a slightly different position in response to the same input pressure. This problem is due to inherent imperfections in the manufacturing or material defects and is common in soft actuators. Using our regulators and a calibration, the variations between actuators could be corrected using only a single pressure supply to the robot. Furthermore, on-board pressure regulators would allow actuators with vastly different pressure requirements to use the same pressure supply.

## V. CONCLUSION

In this paper, we have demonstrated the functionality of pressure regulators that can be used for soft robots. These regulators are designed to be compact enough to be put on-board centimeter-scale soft robots while also giving full control of pressure and allowing for addressability of individual actuators. We revealed basic characteristics of the pressure regulator and demonstrated its ability to follow a desired pressure over time, as well as its ability to respond to disturbances in pressure. Finally, we showed briefly how these regulators can be placed on a soft robot to reduce the number of pneumatic tethers in the system. One impact of this work is that the regulators can be used to account for the variations that typically arise in the manufacture of soft actuators. Additionally, because these regulators can be controlled remotely using I2C communication, they can be scaled to large arrays while maintaining a single pneumatic tether and a single bus of four wires coming from the robot. While not fully untethering a robot, this regulator brings us one step closer to untethered centimeter-scale soft robots by generalizing pressure control in a way that can be easily adapted to on-board pressure generation methods.

## ACKNOWLEDGEMENTS

This work was supported by the National Aeronautics and Space Administration under the Early Career Faculty program (80NSSC17K0553), and by the Office of Naval Research under the Young Investigator Program (N00014-17-1-2604). JCC and DSS are supported by NASA's Space Technology Research Fellowships (Grants NNX15AQ75H and 80NSSC17K0164, respectively). ELW is supported by a National Science Foundation Graduate Research Fellowship (Grant DGE-1333468). We would also like to thank R. Adam Bilodeau for assistance with photos, Robert Shepherd for providing the CAD files for the multi-gait soft robot, and Robert Baines for assistance with manufacturing the robot.

## REFERENCES

[1] M. T. Tolley, R. F. Shepherd, B. Mosadegh, K. C. Galloway, M. Wehner, M. Karpelson, R. J. Wood, and G. M. Whitesides, "A Resilient, Untethered Soft Robot," *Soft Robotics*, vol. 1, pp. 213–223, Aug. 2014.

[2] C. D. Onal and D. Rus, "Autonomous undulatory serpentine locomotion utilizing body dynamics of a fluidic soft robot," *Bioinspiration & Biomimetics*, vol. 8, p. 026003, June 2013.

[3] M. Luo, Y. Pan, E. H. Skorina, W. Tao, F. Chen, S. Ozel, and C. D. Onal, "Slithering towards autonomy: a self-contained soft robotic snake platform with integrated curvature sensing," *Bioinspiration & Biomimetics*, vol. 10, no. 5, p. 055001, 2015.

[4] A. A. Stokes, R. F. Shepherd, S. A. Morin, F. Ilievski, and G. M. Whitesides, "A Hybrid Combining Hard and Soft Robots," *Soft Robotics*, vol. 1, pp. 70–74, July 2013.

[5] C. D. Onal, X. Chen, G. M. Whitesides, and D. Rus, "Soft mobile robots with on-board chemical pressure generation," in *Robotics Research*, pp. 525–540, Springer, 2017.

[6] R. F. Shepherd, A. A. Stokes, J. Freake, J. Barber, P. W. Snyder, A. D. Mazzeo, L. Cademartiri, S. A. Morin, and G. M. Whitesides, "Using Explosions to Power a Soft Robot," *Angewandte Chemie International Edition*, vol. 52, pp. 2892–2896, Mar. 2013.

[7] M. T. Tolley, R. F. Shepherd, M. Karpelson, N. W. Bartlett, K. C. Galloway, M. Wehner, R. Nunes, G. M. Whitesides, and R. J. Wood, "An untethered jumping soft robot," in *2014 IEEE/RSJ International Conference on Intelligent Robots and Systems*, pp. 561–566, Sept. 2014.

[8] N. W. Bartlett, M. T. Tolley, J. T. B. Overvelde, J. C. Weaver, B. Mosadegh, K. Bertoldi, G. M. Whitesides, and R. J. Wood, "A 3d-printed, functionally graded soft robot powered by combustion," *Science*, vol. 349, pp. 161–165, July 2015.

[9] M. Wehner, R. L. Truby, D. J. Fitzgerald, B. Mosadegh, G. M. Whitesides, J. A. Lewis, and R. J. Wood, "An integrated design and fabrication strategy for entirely soft, autonomous robots," *Nature*, vol. 536, pp. 451–455, Aug. 2016.

[10] N. Napp, B. Araki, M. T. Tolley, R. Nagpal, and R. J. Wood, "Simple passive valves for addressable pneumatic actuation," in *Robotics and Automation (ICRA), 2014 IEEE International Conference on*, pp. 1440–1445, IEEE, 2014.

[11] "Custom circuit board." <https://github.com/the-faboratory/PressureServoCircuitBoard>.

[12] "Fluidic control board." <https://softroboticstoolkit.com/book/control-board>. Accessed: 2017-12-07.

[13] "Valve terminal cpv14-vi." [https://www.festo.com/net/ro\\_ro/SupportPortal/default.aspx?q=cpv14-vi+atex&tab=3](https://www.festo.com/net/ro_ro/SupportPortal/default.aspx?q=cpv14-vi+atex&tab=3). Accessed: 2017-12-07.

[14] "Itv series catalog." <http://www.smc-pneumatics.com/pdfs/ITV.pdf>. Accessed: 2018-1-19.

[15] M. A. Robertson, H. Sadeghi, J. M. Florez, and J. Paik, "Soft Pneumatic Actuator Fascicles for High Force and Reliability," *Soft Robotics*, vol. 4, pp. 23–32, Oct. 2016.

[16] "X-valve - miniature pneumatic solenoid valve." <http://ph.parker.com/us/12051/en/x-valve-miniature-pneumatic-solenoid-valve>. Accessed: 2017-12-07.

[17] "Ten-x - miniature pneumatic solenoid valve." <http://ph.parker.com/us/12051/en/ten-x-miniature-pneumatic-solenoid-valve>. Accessed: 2017-12-07.

[18] R. F. Shepherd, F. Ilievski, W. Choi, S. A. Morin, A. A. Stokes, A. D. Mazzeo, X. Chen, M. Wang, and G. M. Whitesides, "Multigait soft robot," *Proceedings of the National Academy of Sciences*, vol. 108, pp. 20400–20403, Nov. 2011.